Electrochimica Acta 56 (2011) 2832–2836

Contents lists available at ScienceDirect

Electrochimica Acta

journal homepage: www.elsevier.com/locate/electacta

Novel nanotextured microelectrodes: Electrodeposition-based fabrication and their application to ultrasensitive nucleic acid detection

Xuping Sun*, Yonglan Luo, Fang Liao, Wenbo Lu, Guohui Chang

Chemical Synthesis and Pollution Control Key Laboratory of Sichuan Province, School of Chemistry and Chemical Industry, China West Normal University, Nanchong 637002, Sichuan, China

ARTICLE INFO

Article history:
Received 16 October 2010
Received in revised form
15 December 2010
Accepted 20 December 2010
Available online 27 December 2010

Keywords:
Microelectrode
Nanotexture
Electrodeposition
Ultrasensitive nucleic acid detection

ABSTRACT

Microelectrodes have become well-established tools in a wide range of analytical studies and applications because they exhibit many cardinal advantages bestowed by their micrometer-sized dimensions over conventional large-surface-area electrodes. Nanostructures display quite unique properties different greatly from those of the bulk materials and are widely used in the field of electroanalysis. Nanotextured microelectrodes (NTMEs) are expected to combine attributes of nanostructures with microelectrodes. In this paper, electrodeposition technique, in combination with well-established microfabrication techniques, is used for the first time to the controllable fabrication of novel Pd, Pt, and Au NTMEs. The use of such NTMEs as a novel platform for ultrasensitive nucleic acid detection is also demonstrated.

The miniaturization of electrochemical systems for applications has received considerable attention of researchers for many years and continues to be a major trend in the field of analytical and bioanalytical chemistry [1], one of the main reasons for which is the down-scaling in size will provide increased sensitivity [2]. However, miniaturization often causes decrease of both the rate of electrochemical conversion and the signal-to-noise ratio. From the point of view of miniaturization it should be noted that the dimensions of electrodes can be reduced from the mm to the μm scale without deteriorating the signal-to-noise characteristics [1]. Microelectrodes are just such kind of electrodes with characteristic dimensions on the micrometer or sub-micrometer scale and offers many cardinal advantages over conventional large-surface-area electrodes such as faster double-layer charging, reduced ohmic loss, high mass-transport rates, and high current intensity, etc. [3,4]. Indeed, recent years have witnessed their rapid development and such electrodes have become well-established tools in a wide range of analytical studies and applications [5,6]. Up to date, many approaches have been successfully used to fabricate microelectrodes, however, the development of a simple but versatile route for the controllable fabrication of such electrodes is still a challenge [7].

Compared to their bulk counterparts, nanostructures exhibit quite unique properties which are heavily depended on their size and shape, and as a result, size and shape-controlled synthesis of such structures has always been a hot research topic [8]. It is also well-established that nanoparticles-modified electrodes can exhibit several unique advantages over conventional macroelectrodes such as enhancement of mass transport, catalysis, high effective surface area and control over electrode microenvironment [9], and the great applications of nanostructures for electroanalysis have been largely reported [10]. For example, boron doped diamond microelectrodes modified by electrodeposition of platinum nanoparticles have been used for the oxidative determination of As(III) at levels below 1 ppb [11]. So it is reasonable to believe that nanotextured microelectrodes (NTMEs) will combine the merits of both microelectrodes and nanostructures for electroanalysis and especially bioelectroanalysis applications. However, to the best of our knowledge, until now, no attention has been paid to the simple fabrication of such kind of novel microelectrodes. In this paper, the widely-used electrodeposition method [12], in combination with well-established microfabrication techniques, is used for the first time to develop a general approach for the fabrication of novel NTMEs, carried out by electrodeposition of Pd, Pt, or Au starting from the bottom of a 500-nanometer pore pre-fabricated by microfabrication technology. The use of such NTMEs as a novel platform for ultrasensitive nucleic acid detection is also demonstrated.

The 500-nm pore used for growing NTMEs by electrodeposition was fabricated using the following four-step procedures: (1) A thick silicon dioxide insulating layer was thermally grown on a silicon wafer. (2) Gold patterns were created on the substrate using electron-beam assisted gold deposition and a standard lift-

* Corresponding author.
E-mail address: sun.xuping@hotmail.com (X. Sun).

0013-4686/$ – see front matter © 2010 Elsevier Ltd. All rights reserved.
doi:10.1016/j.electacta.2010.12.065

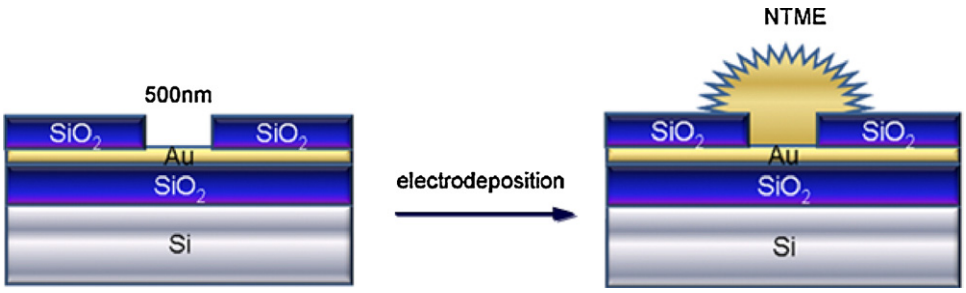

Scheme 1. A schematic drawing to illustrate the fabrication process of the NTME.

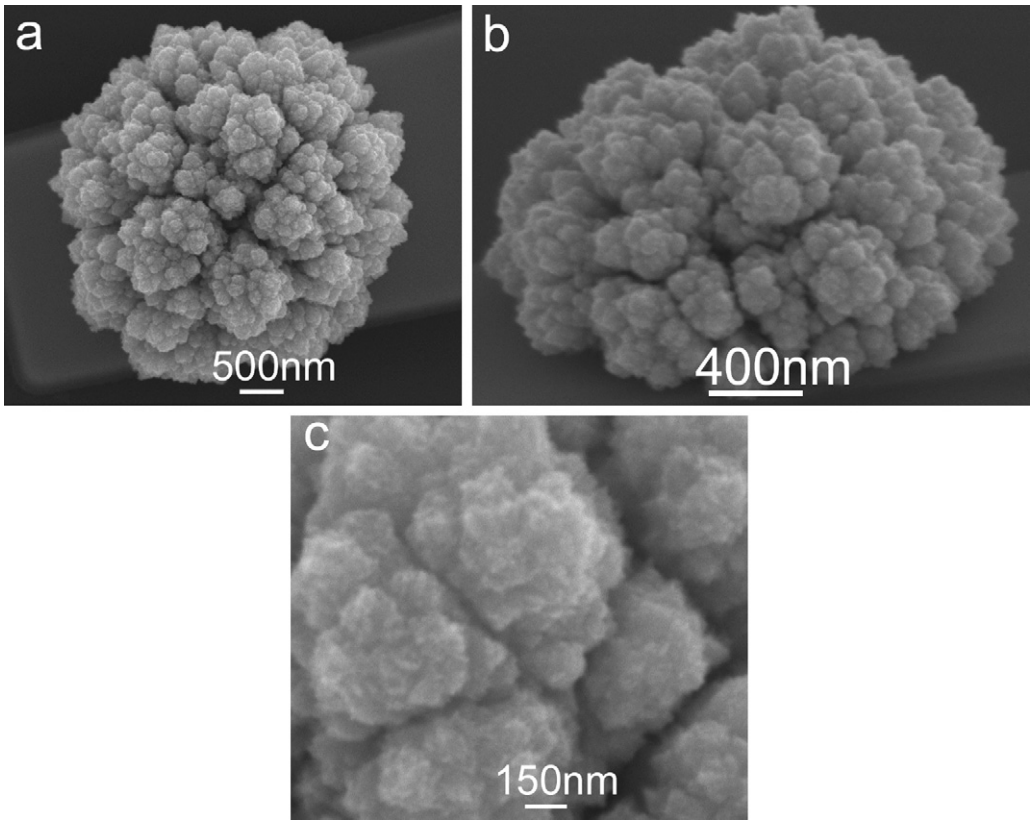

Fig. 1. (a) Top-view and (b) 66° tilted-view SEM images of the Pd NTME thus fabricated, and (c) a local view the Pd NTMEs surface.

off process. (3) A silicon dioxide dielectric layer with a thickness of 500 nm was then deposited on the gold pattern using plasma-enhanced chemical vapor deposition (PECVD). (4) Openings about 500 nm in diameter were imprinted through the dielectric exposing the underlying gold electrode. Electrodeposition and electrochemical studies were performed using BAS Bioanalytical Systems (BAS CV-50W analyzer) in a three-electrode configuration at room temperature with the use of a Ag/AgCl electrode equipped with a Luggin capillary as the reference electrode and a platinum wire as the counter electrode. Pd NTMEs were fabricated by electrodeposition from an aqueous solution containing 4.5 mM of the corresponding metal salt solution (H_2PdCl_4) and 0.5 M of the supporting electrolyte (HCl) at −100 mV for 200 s by single potential time base mode, with the use of the 500 nm opening of gold substrate as the working electrode. Scheme 1 shows a schematic drawing to illustrate the fabrication process of the NTME.

Scanning electron microscopy (SEM) measurements were made on a HITACHI S-3400N microscope operated at an accelerating voltage of 10 kV. The ss-thiolated-DNA probes were immobilized on Pd NTMEs. The NTMEs were exposed to a solution of 5 μM SH-DNA in 25 mM sodium phosphate/25 mM NaCl (pH 7) containing 20 mM $MgCl_2$ in a humidity chamber at room temperature for 1.5 h, and then rinsed in 25 mM sodium phosphate/25 mM NaCl (pH 7). The chemisorption of DNA onto electrodes was confirmed by scanning from 0 to 500 mV in a solution of 2 mM $Fe(CN)_6^{3-}$ in 25 mM sodium phosphate (pH 7)/25 mM NaCl at a scan rate of 100 mV/s. Electrodes were then rinsed in 25 mM sodium phosphate/25 mM NaCl (pH 7) and electrocatalysis currents were measured as described below. A solution of 10 pM target DNA in 25 mM sodium phosphate/25 mM NaCl (pH 7) containing 100 mM $MgCl_2$ was then introduced in a thermostatted humidity chamber at 37–40 °C and 1 h was used for the hybridization experiment. Electrocatalytic current was then remeasured as described below. Electrocatalytic currents were measured using in solutions of 4 mM $Fe(CN)_6^{3-}$ and 10 μM $Ru(NH_3)_6^{3+}$ in 25 mM sodium phosphate/25 mM NaCl (pH 7) at a scan rate of 50 mV/s. Catalytic current change due to the hybridization event (ΔI) was calculated as follows:

$$\Delta I\,\% = \frac{I_{\text{final}} - I_{\text{initial}}}{I_{\text{initial}}} \times 100$$

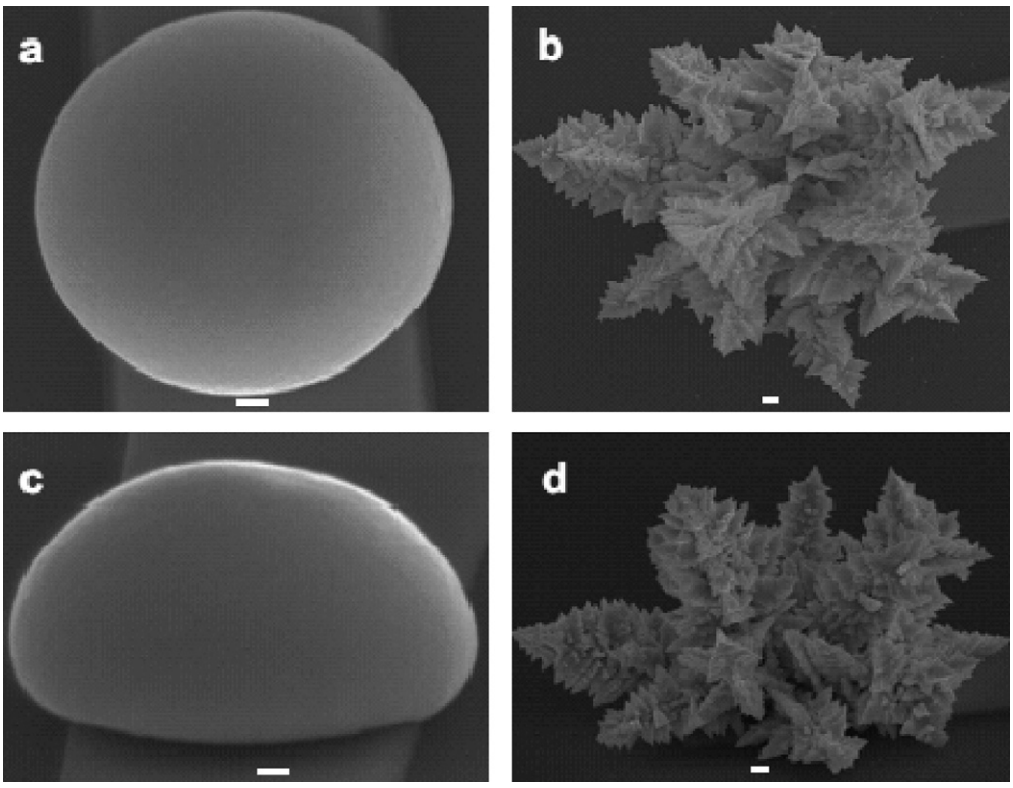

Fig. 2. Top-view SEM image of (a) Pt and (b) Au NTMEs obtained at −100 mV for 200 s with the use of HCl as supporting electrolyte, the corresponding 66° tilted-view SEM image is shown in c and d, respectively (scale bar: 500 nm).

where I_{final} and $I_{initial}$ correspond to current signal after and before the hybridization, respectively.

Fig. 1a and b shows the top-view and 66° tilted-view SEM images of the Pd NTME thus fabricated. It is seen that a cauliflower-shaped microstructure about 4.2 and 2.2 μm and in diameter and height, respectively, was formed at the potential applied. A local view the electrode surface reveals its nano-roughed nature, as shown in Fig. 1c. All these observations clearly indi-

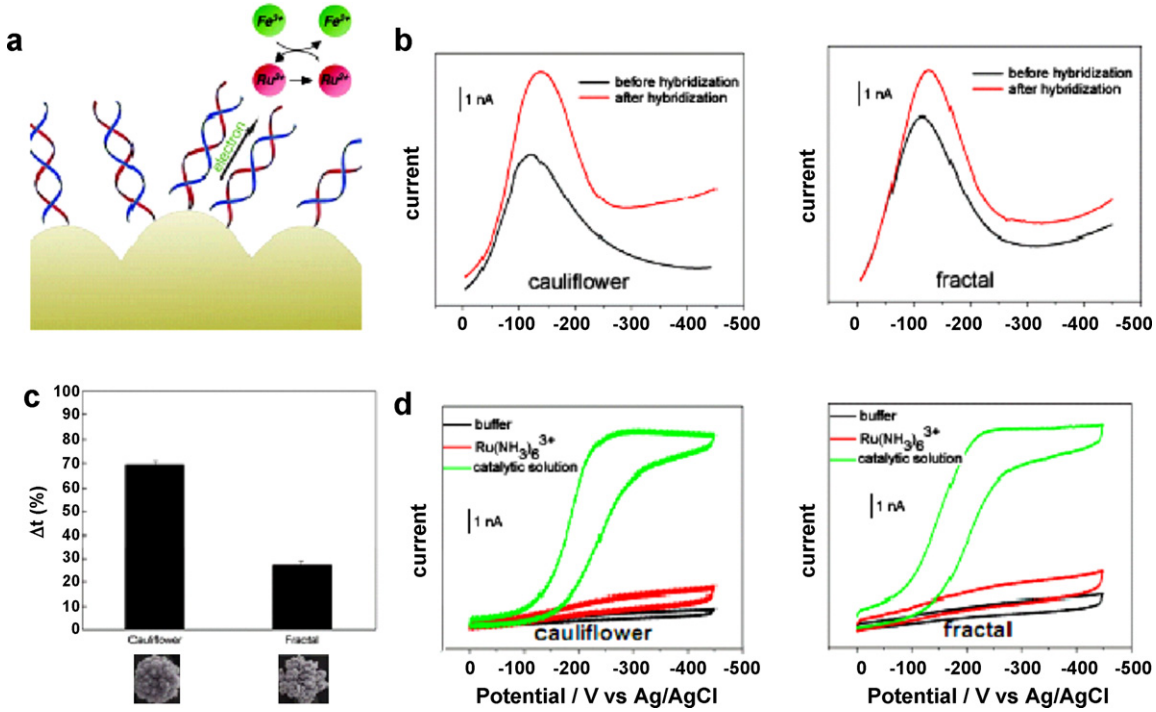

Fig. 3. (a) A schematic illustration of Ru(III)/Fe(III) electrocatalysis at a DNA-modified, nano-roughed Pd NTMEs. (b) Detection of target DNA through changes in catalytic current measured by DPV technique. (c) Hybridization efficiency of target DNA at cauliflower and fractal Pd NTMEs. (d) CVs of these two Pd NTMEs after hybridization in solution of buffer only, $Ru(NH_3)_6^{3+}$ in buffer, and catalytic solution in buffer.

cate the formation of Pd microelectrode with nano-roughed texture.

The versatile nature of our NTMEs system is further explored by performing electrodeposition of Pt and Au. Fig. 2 shows top-view SEM image of (a) Pt and (b) Au structures obtained at −100 mV for 250 s with the use of HCl as supporting electrolyte, and the corresponding 66° tilted-view SEM image is also shown in Fig. 2c and d, respectively. It is clearly seen that Pt and Au microelectrodes are also formed. It is quite interestingly found that semispherical Pt NTME with smooth surface was obtained. The diameter and height of Pt NTMEs is measured to be about 6.1 and 3.8 μm, respectively. However, the same deposition conditions give tree-like fractal Au microstructure about 21 μm in diameter and 5.5 μm in height. A close view of the Au NTMEs further indicates that the "leaf" of such tree is nanoscale in size and triangular in shape. All the above observations indicate that the shape of the NTMEs can be affected by the type of metal ions used.

The use of as-fabricated NTMEs as a novel kind of platform for electrochemical DNA detection has also been preliminarily investigated by choosing Pd NTMEs as proof-of-concept demonstration. For comparative study of hybridization efficiency of DNA at such NTMEs, we tested two kinds of Pd NTMEs with different geometry, that is, cauliflower and fractal formed at deposition potential of −100 mV and −250 mV, respectively, as a biosensing platform using an electrocatalytic DNA detection method d. This label-free system reports on the binding of a target DNA sequence to an immobilized probe oligonucleotide using a catalytic reaction between two transition-metal ions, $Ru(NH_3)_6^{3+}$ and $Fe(CN)_6^{3-}$. The Ru(III) electron acceptor is reduced at the electrode surface and then reoxidized by excess Fe(III), which makes the electrochemical process catalytic. The increased concentration of anionic phosphates at the electrode surface that accompanies DNA hybridization increases the local concentration of $Ru(NH_3)_6^{3+}$, and therefore produces large changes in the electrocatalytic signal. This approach works with sequences of varied composition and is thus widely applicable to any target gene of interest. In the present study, a single-stranded probe DNA was thiolated and covalently attached to Pd NTME through a Pd–thiol bond [13]. Fig. 3a shows a schematic illustration of Ru(III)/Fe(III) electrocatalysis at a DNA-modified, nanoroughed Pd NTMEs. To study hybridization efficiency, each DNA-modified Pd NTMEs was analyzed using Ru(III)/Fe(III) electrocatalysis before and after the hybridization of target sequences. Fig. 3b shows the detection of complementary target sequences through changes in catalytic current measured by differential pulse voltammetry (DPV) technique at probe-modified cauliflower and fractal Pd NTMEs due to the occurrence of hybridization event. Obviously, current signal increases upon hybridization were observed for both NTMEs (concentration of target DNA: 10 pM). Note that no signal change was observed for the probe-modified NTMEs toward non-complementary target sequences, indicating that the change in catalytic current in our present system is indeed due to the base pairing between probe and its target, excluding the nonspecific target binding. It was reported that the efficiency of an electrocatalytic process should be strongly influenced by the rate of diffusion [11]. Given that these two NTMEs exhibit different nanotexturing and thus provide different nanoenvironment to the DNA molecules involved in this system, it is reasonable to conclude that different diffusion behavior and rate of DNA towards the cauliflower and fractal Pd NTMEs may be expected, and therefore, different hybridization efficiency was observed. Another possible reason for such difference may be due to the formation of the film of probe DNA with different density film at such two different kinds of Pd NTMEs. It is worthwhile pointing out that cauliflower Pd NTME is expected to permit much more efficient target capture than its fractal counterpart, leading to bigger change of current signal, as shown in Fig. 3c. The relative standard deviation (RSD) of the

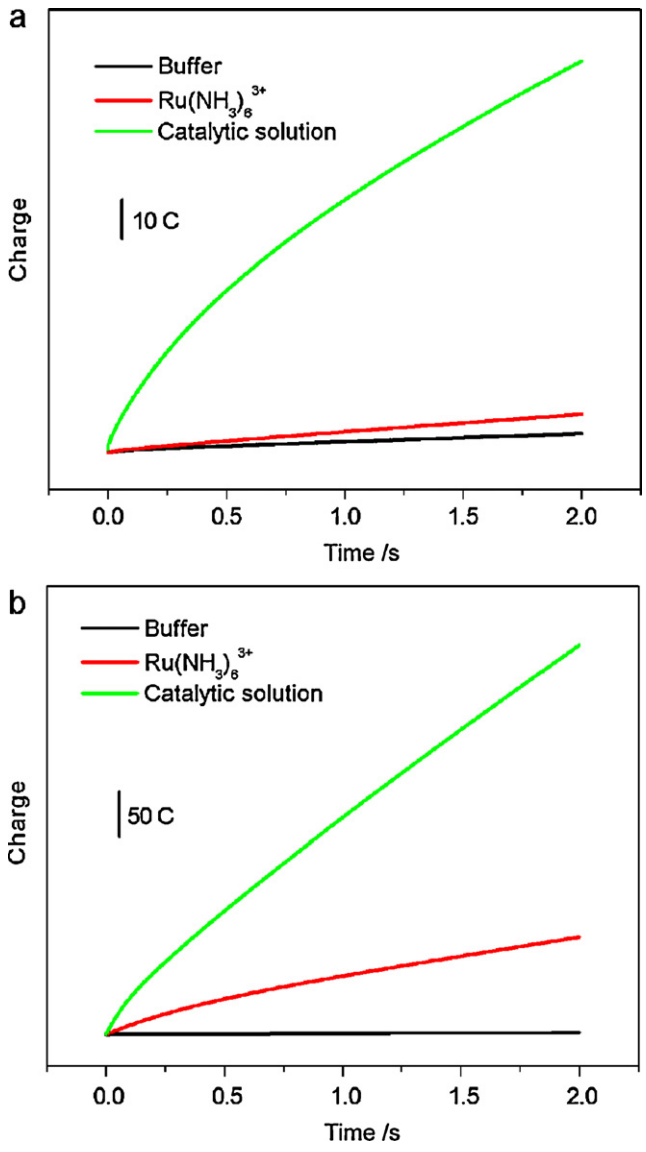

Fig. 4. Chronocoulometry data of (a) cauliflower and (b) fractal Pd NTMEs after hybridization in solution of buffer only, 10 μM $Ru(NH_3)_6^{3+}$ in buffer, and catalytic solution containing 10 μM $Ru(NH_3)_6^{3+}$ and 4 mM $Fe(CN)_6^{3-}$ in buffer.

amperometric responses of probe-modified cauliflower and fractal Pd NTMEs to 10 pM complementary target sequences are about 2.5% and 3.5% for 5 measurements, respectively, indicating the good reproducibility of this detection system. Fig. 3d shows the cyclic voltammetries (CVs) of these two Pd NTMEs after hybridization in solution of buffer only, $Ru(NH_3)_6^{3+}$ in buffer, and catalytic solution in buffer, and the big change of current clearly confirms that $Fe(CN)_6^{3-}$ also effectively catalyzes the electrochemical redox reaction of the $Ru(NH_3)_6^{3+}/Ru(NH_3)_6^{2+}$ couple in the present system. We have performed one control experiment by using one regular planar electrode as the sensing platform at the same conditions and found that the change of current signal after the hybridization event is only about 5% of that obtained on cauliflower Pd NTME. This observation clearly indicates that the NTME has the advantage of increasing largely the detection sensitivity.

To further calculate the turnovers per $Ru(NH_3)_6^{3+}$, we did chronocoulometry experiment at these two Pd NTMEs after hybridization in solution of buffer only, $Ru(NH_3)_6^{3+}$ in buffer, and catalytic solution in buffer (Fig. 4). When a cauliflower Pd NTMEs was used, eighteen turnovers were observed per $Ru(NH_3)_6^{3+}$, how-

ever, when a fractal Pd NTMEs was used under the same conditions, only four turnovers were observed per $Ru(NH_3)_6^{3+}$. These results suggest that better accessibility of the redox-active ions is provided by the cauliflower Pd structure.

In summary, the combination of microfabrication techniques and electrodeposition method has been proven for the first time to be an effective strategy for fabricating a novel kind of nanotextured microelectrodes. The use of such electrodes for ultrasensitive DNA detection by electrochemical method was also successfully demonstrated. The nanotexting dramatically increases the active surface area of the electrode and thus electroactivity [14]. which is crucial to high signal-to-noise ratio [15], and on the other hand, the nanostructures at the surface can act as "electron antennae" to effectively realize the direct electron transfer between the electrode and the deeply buried electroactive center of enzyme [16], and therefore, such kind of microelectrodes also may hold great promise as a new "sensitive" platform for detecting enzyme.

References

[1] F.M. Matysik, Miniaturization of Electroanalytical Systems, Springer-Verlag, 2002.
[2] R. Szamocki, et al., Anal. Chem. 79 (2007) 533.
[3] A.M. Bond, K.B. Oldham, C.G. Zoski, Anal. Chim. Acta 216 (1989) 177.
[4] J. Heinze, Angew. Chem. Int. Ed. 32 (2003) 1268.
[5] A.J. Bard, Electrochemical Methods: Fundamentals and Applications, Wiley, New York, 2001.
[6] C.E. Reimers, Chem. Rev. 107 (2007) 590.
[7] C.G. Zosic, Handbook of Electrochemistry, Elsevier, 2007.
[8] C. Burda, X. Chen, R. Narayanan, M.A. El-Sayed, Chem. Rev. 105 (2005) 1025.
[9] E. Katz, I. Willner, J. Wang, Electroanalysis 16 (2004) 19.
[10] C.M. Welch, R.G. Compton, Anal. Bioanal. Chem. 384 (2006) 601.
[11] S. Hrapovic, Y. Liu, J.H.T. Luong, Anal. Chem. 79 (2007) 500.
[12] E.J. Menke, et al., Nat. Mater. 5 (2006) 914.
[13] C.K. Yee, R. Jordan, A. Ulman, H. White, A. King, M. Rafailovich, J. Sokolov, Langmuir 15 (1999) 3486.
[14] Z. Li, V. Ravaine, S. Ravaine, P. Garrigue, A. Kuhn, Adv. Funct. Mater. 17 (2007) 618.
[15] R. Szamocki, et al., Angew. Chem. Int. Ed. 45 (2006) 1317.
[16] K.R. Brown, A.P. Fox, M.J. Natan, J. Am. Chem. Soc. 118 (1996) 1154.